Journal of Structural Geology, Vol. 5, No. 3/4, pp. 299 to 305, 1983
Printed in Great Britain

0191-8141/83 $3.00 + 0.00

Spatial integration of strains using finite elements

PETER ROBERT COBBOLD and MARIE-NOËL PERCEVAULT

Centre Armoricain d'Etude Structurale des Socles (CNRS), Université de Rennes,
35042 Rennes Cedex, France

(*Received* 7 *July* 1982; *accepted in revised form* 13 *December* 1982)

Abstract—The finite element method for spatial integration of strains was conceived and then evolved as an intuitively reasonable means of calculating the pretectonic shape of a region. Here we show that the technique is basically an improved Euler method for integrating differential equations, and that unstrained elements (parallelepipeds) should therefore be fitted together so that face centres of adjoining elements coincide; or where this is not possible, the interfacial distances should be minimized. Minimization yields the translation and rotation an element must undergo in order to fit well into the hole enclosed by neighbouring elements. Techniques are described for fitting of an array of elements by computer. A fastpacking routine gives a good but approximate result; whereas a slower but more rigorous procedure enables the result to be improved. Finally, a short discussion of errors is given.

INTRODUCTION

AS STRAIN data measured across tectonic structures become more abundant, there is growing interest in using them to calculate pretectonic shapes. This can be done by spatially integrating the strains to obtain the deformation field. Thus, Ramsay & Graham (1970) showed that the amount of simple shear can be integrated across a shear zone to yield the total shear displacement. Similarly Hossack (1978) suggested that stretch can be integrated along a strain trajectory to yield the original length of that line.

For general plane strain fields, Oertel (1974) introduced the practical idea of triangular domains within each of which strain is homogeneous. The idea was further explored by Schwerdtner (1977), who used square domains and showed that, after unstraining, the resulting parallelograms must be translated and rotated before they will fit together without large gaps and overlaps. The fitting procedure was done by hand, using pieces of paper for unstrained domains and pins to fix them into position.

Cobbold (1979) observed that such domains were equivalent to finite elements, as used in mechanical problems, and introduced a numerical procedure for minimizing gaps and overlaps between planar elements, so enabling them to be fitted more efficiently and more objectively. At that time, the use of rectangular elements parallel to strain trajectories was advocated, as a means of simplifying the mathematics; but recent developments indicate that the basic mathematics can be presented in a simple form, independent of the choice of element shape, and valid for three-dimensional situations, as well as two-dimensional ones.

The object of the present paper is to justify the use of finite elements on mathematical grounds. This leads to ideas about how elements should fit together and to a general method for minimizing gaps and overlaps. Finally, there is a short discussion of errors.

MATHEMATICAL BASIS FOR USING FINITE ELEMENTS

The mathematical problem

If the Cartesian coordinates of a material point are $\mathbf{Z}$ for the undeformed state and z for the deformed state, then the deformation (Truesdell & Toupin 1960, p. 243) is represented by the transformation

$$z = z(\mathbf{Z}), \tag{1}$$

where the bold-face characters indicate vector or tensor quantities.

Similarly, the inverse,

$$\mathbf{Z} = \mathbf{Z}(z), \tag{2}$$

will be called here the reverse deformation. The mathematical problem is to obtain (1) and (2), given other information. Suppose, first of all, that at each point in the deformed state, z, we are given the reverse deformation gradients, that is, the nine Cartesian components,

$$\frac{\partial Z_I}{\partial z_j} = Z_{I,j}, \quad (I, j = 1, 2, 3) \tag{3}$$

as functions of position, z. Equations (3) are then nine partial differential equations in three unknowns, the Z_I. By integrating them, we can in theory, obtain (1) and (2) and so solve the problem; to be integrable, however, the reverse deformation gradients must satisfy six conditions of compatibility,

$$\frac{\partial}{\partial z_k}\left(\frac{\partial Z_I}{\partial z_j}\right) = \frac{\partial}{\partial z_j}\left(\frac{\partial Z_I}{\partial z_k}\right), \tag{4}$$

otherwise the answer will not be unique.

In real geological problems, there is no guarantee that data will be free from errors and that the compatibility conditions, (4), will be perfectly satisfied. What is required, therefore, is a flexible method of integration

that can overcome problems of incompatibility between the data. Simple numerical methods will be explored first, as they provide a mathematical basis for the use of finite elements.

The Euler method and modified Euler method

The Euler and modified Euler methods are well known as approximate numerical methods for solving ordinary differential equations, such as

$$\frac{dy}{dx} = f'(x), \tag{5}$$

of which the integral is

$$y = \int f'(x)dx = f(x). \tag{6}$$

If we are given values of $f'(x)$ for all values of x, then the simplest numerical method of integration is the Euler method. The range of x values is divided into equal step intervals, Δx. The gradient $f'(x)$ is taken to be constant at the beginning of each step interval and projected forward throughout that interval (Fig. 1a). By taking a number of successive forward steps, an approximate solution is built up and its graphical form is known as the Cauchy polygon. Although the Euler method is the simplest, it is not very accurate.

The modified Euler method results in much greater accuracy at the expense of a very small modification. The range of x values is divided into equal step intervals, as before, but the gradient, $f'(x)$, is taken in the middle of a step interval and projected forwards and backwards through half a step interval (Fig. 1b). The approximate solution is then built up by moving forwards or backwards through a number of successive steps.

In both methods of solution, the accuracy improves as the step interval decreases until, in the limit where the step interval vanishes, the exact answer is always obtained. For finite step intervals, however, we may ask if there are any particular functions (6) for which an exact integral is always obtained, no matter how large the step interval. The answer is yes. For the Euler method, this will be so if y is a linear function of x, so that its gradient is constant across all step intervals, and the graph of y vs x is a straight line. Under these conditions, but only under these conditions, points on the Cauchy polygon also lie along the exact integral. For the modified Euler method, an exact solution is obtained, not only for a linear function of x, but also for a quadratic function (Fig. 1b). This illustrates the improvement provided by the modified Euler method; it will give the exact answer if the gradient, $f'(x)$, is a linear function of position and will give a very good answer for more complex functions.

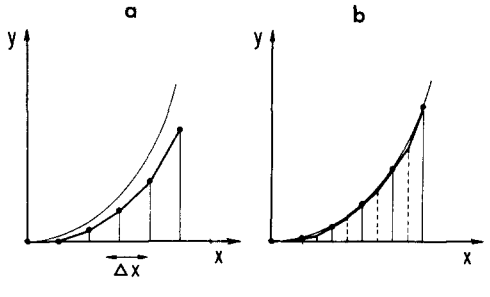

Fig. 1. Numerical integration of an ordinary differential equation. Thin curve represents function $y = x^2$, which is exact integral of $dy/dx = 2x$, with $y = 0$ when $x = 0$. (a) Euler method of integration, showing estimated values of y (dots) and slope dy/dx (thick straight line segments, forming Cauchy polygon) at beginning of each step interval, Δx. (b) Modified Euler method. Slopes dy/dx (thick segments) are projected forward and backward over half a step interval. Estimated values of y (dots) fall exactly on curve $y = x^2$.

THE FINITE ELEMENT METHOD

Suppose now that we apply a modified Euler method to integrate the partial differential equations (3). By analogy with what is done for ordinary differential equations, equal step intervals are taken in all three (or two) directions, z_i, in the deformed state. This defines an array of finite elements which are, in fact, cubes (or squares, Fig. 2a). The reverse deformation gradients are taken at the centroid of each element and assumed constant within it. Thus, it is a simple matter to undeform each element, using the theory of homogeneous strain. On doing so, we find that the elements become parallelepipeds (or parallelograms, Fig. 2b) and that gaps and overlaps appear between them. To build up the solution along each of the directions z_i, we bring the face centres of adjacent elements once again into coincidence by translating them rigidly (Fig. 2c). The new positions, Z_I, of the element centroids represent the numerical solution of the problem.

By analogy with what happens for ordinary differential equations, we might suspect that the finite element method, being a modified Euler method, gives the exact solution if (2) is a quadratic function. This is indeed so, as illustrated by the two-dimensional model (Fig. 3),

$$\begin{aligned} Z_1 &= z_1 + 0.1z_1^2 - 0.2z_1z_2 + 0.2z_2^2, \\ Z_2 &= z_2 + 0.1z_1^2 + 0.3z_1z_2 - 0.1z_2^2, \end{aligned} \tag{7}$$

which is isochoric (no volume change). Notice that all pairs of face centres can be brought simultaneously into coincidence, whereupon the element centroids (but no other points) are exact positions in the undeformed state. Notice, furthermore, that pairs of element corners are far from coincident: this is simply a result of the finite size of the elements and does not indicate errors in data or in the solution, as stated mistakenly in earlier publications (Percevault & Cobbold 1982).

Now suppose that the function (2) can be expressed as a power series with terms of higher order than 2. Even if the reverse deformation gradients are given exactly at the element centroids, can all pairs of face centres be made to coincide as in the quadratic model (Fig. 3)? The answer is no, because numerical errors can build up differently in different directions, leading to local incompatibilities. Errors in the reverse deformation gradients may make this problem worse; or they may, by chance,

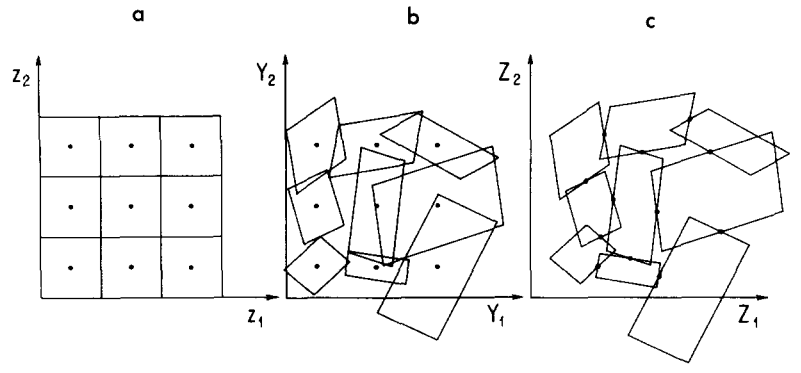

Fig. 2. Integration of reverse deformation gradients using finite elements. (a) Initial grid of square elements. (b) Undeformed elements, in original positions. (c) Same undeformed elements, in new positions such that face centres coincide.

make it better; but in any case, it is necessary to relax the stringent requirement that pairs of face centres coincide absolutely. Instead it is reasonable to introduce a method of minimizing interfacial distances (distances between pairs of face centres), as done in the following section.

Before going on to this however, let us consider a problem, geologically more realistic, where the reverse deformation gradients are not known completely, but instead only the strains are known. This leaves the rigid rotations to be determined, as well as the translations. Fortunately, a rigid rotation does not change the shape of an element. Therefore, the same method of integration can be applied, provided it includes a minimization of interfacial distances. This is a great advantage of the finite element method.

By considering the finite element method as equivalent to a modified Euler method of integration, it has been suggested that all elements in the deformed state should be identical cubes (or squares), so as to ensure equal and regular step intervals in all directions. This restriction is, in practice, not always necessary, nor does it always guarantee that errors will be minimal. Instead there is some justification for locally reducing element size where strain gradients are largest, and for making element boundaries coincide as much as possible with surfaces of discontinuity in the strain field (such as boundaries between layers of different rheological properties). In practice, we advocate using roughly equant parallelepipeds and making up an array such that face centres of adjoining elements coincide.

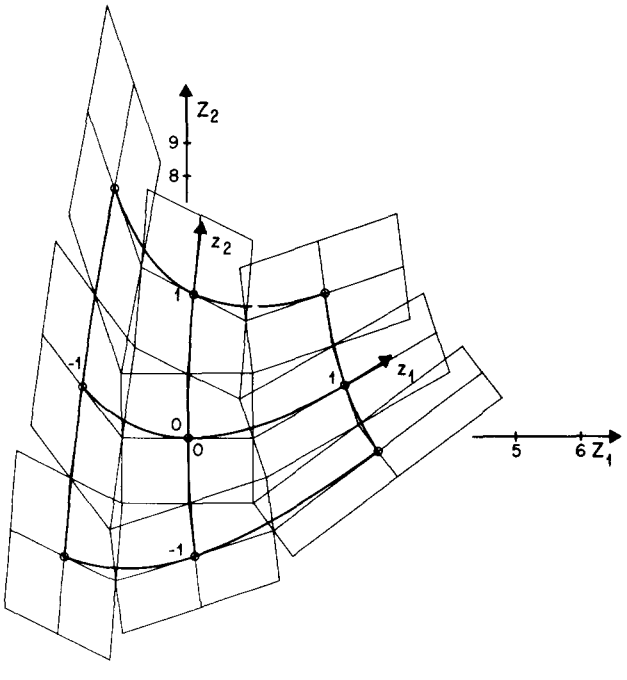

Fig. 3. Quadratic model of deformation, showing new coordinates (Z_1, Z_2), old coordinates (z_1, z_2) now undeformed, and undeformed elements positioned so that face centres coincide. Notice that element centroids fall on coordinate curves, z_1, z_2.

FITTING OF FINITE ELEMENTS

Deviation of an element from its hole

A consequence of using elements of finite size and of errors in strain data is that, once strains have been removed, an element need not have the same shape as the hole enclosed by its immediately adjacent neighbours. We shall now define the deviation of an element from its hole and then minimize it to obtain the best fit. A brief mathematical discussion of this procedure was given by Cobbold (1979) for two-dimensional problems. Here we will give a more general three-dimensional analysis.

Consider an element defined by points z on its boundary in the deformed state. In the undeformed state, the element is defined by boundary points $\boldsymbol{Z}$; and the hole it occupies, by boundary points $\boldsymbol{Z}^*$. Furthermore, in an intermediate state, the boundary points are $\boldsymbol{Y}$ and $\boldsymbol{Y}^*$ (Fig. 4).

The deviation, $\mathscr{D}$, of the element from its hole, in the intermediate state, is defined as

$$\mathscr{D} = \frac{1}{n}\sum_{1}^{n} |\boldsymbol{Y}^* - \boldsymbol{Y}|^2 = \overline{(Y_I^* - Y_I)^2}, \qquad (8)$$

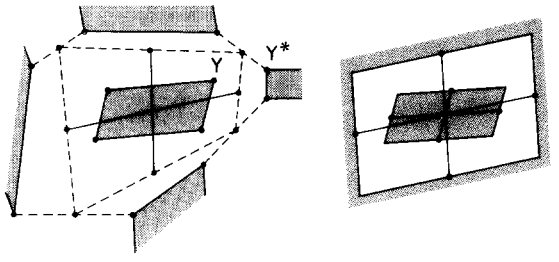

Fig. 4. An element within its true hole (left) and its equivalent hole (right). Element (shaded parallelogram) has corner $\boldsymbol{Y}$. Neighbouring element (shaded, shown in part) has corner $\boldsymbol{Y}^*$.

where n is the number of boundary points considered and the bar indicates an arithmetic mean. A similar definition was used by Grioli (1940) for analysing the deviation of one deformation from another; but he considered all points on the boundary of a sphere and therefore used a volume integral instead of the summation in (8).

The deviation, $\mathscr{D}$, is defined as a mean-square distance and therefore can be minimized directly, as in any least-mean-square procedure.

Minimization with respect to unknown translation

Suppose that in passing from the intermediate to the undeformed state, the hole is rigid and stationary, whereas the element undergoes a rigid translation only. This is expressed mathematically as

$$\begin{aligned} \boldsymbol{Y}^* &= \boldsymbol{Z}^*, \\ \boldsymbol{Y} &= \boldsymbol{Z} + \boldsymbol{B}, \end{aligned} \tag{9}$$

where $\boldsymbol{B}$ is a translation vector. Substitution of (9) into (8) yields

$$\mathscr{D} = \overline{(Z_I^* - Z_I - B_I)^2}. \tag{10}$$

To minimize (10), differentiate with respect to the unknown translation and set the result equal to zero:

$$\frac{\partial \mathscr{D}}{\partial B_I} = 2\overline{(Z_I^* - Z_I - B_I)} = 0. \tag{11}$$

As $\boldsymbol{B}$ is assumed constant over the element, (11) can be written

$$B_I = \overline{Z_I^*} - \overline{Z_I}. \tag{12}$$

Here $\overline{Z_I}$ is the vector mean of points around the element and $\overline{Z_I^*}$ the vector mean of points around the hole. To minimize the deviation, $\mathscr{D}$, the element must be translated until these vector means coincide. A similar result, in less general form, was given by Etchecopar (1974).

Minimization with respect to unknown rotation

Suppose that $\mathscr{D}$ has already been minimized with respect to element translation so that $\overline{Y_I^*} = \overline{Y_I}$. Clearly a rigid rotation about this vector mean will not change its position, so that previous results will be conserved. To simplify the mathematics write, for example,

$${}_0Y_I = Y_I - \overline{Y_I}, \tag{13}$$

where ${}_0Y_I$ is the deviation of Y_I from the mean value, $\overline{Y_I}$. A rigid rotation of the element about Y_I and within a stationary rigid hole is expressed as

$$\begin{aligned} {}_0Y_I^* &= {}_0Z_I^*, \\ {}_0Y_I &= R_{IJ0}Z_J, \end{aligned} \tag{14}$$

where R_{IJ} is the rotation tensor. Substitution of (14) into (8) yields

$$\mathscr{D} = \overline{({}_0Z_I^* - R_{IJ0}Z_J)^2} = \overline{({}_0Z_I^*)^2} + \overline{({}_0Z_J)^2} - 2R_{IJ0}\overline{Z_I^*{}_0Z_J}. \tag{15}$$

The first two terms on the right hand side of (15) are invariant with respect to rotation, whereas, in the third term, the quantity $\overline{{}_0Z_I^*{}_0Z_J}$ is invariant. The deviation is a minimum when $\overline{{}_0Z_I^*{}_0Z_J}$ is a maximum. Also, no rotation occurs if $R_{IJ} = \delta_{IJ}$ the unit tensor, whereupon $\overline{{}_0Z_I^*{}_0Z_J}$ contracts to become its trace, $\overline{{}_0Z_I^*{}_0Z_I}$. But the trace of a tensor is a maximum if the latter is symmetric; therefore we conclude that $\mathscr{D}$ is a minimum with respect to rotation when $\overline{{}_0Z_I^*{}_0Z_J}$ is symmetric. If it is not symmetric, it can be expressed as the product of symmetric and orthogonal components. The orthogonal component is the inverse of the rotation that renders $\overline{{}_0Z_I^*{}_0Z_J}$ symmetric and so minimizes $\mathscr{D}$. An efficient and reliable numerical method of decomposing an asymmetric matrix is given in the Appendix.

Minimization with respect to unknown further strain and rotation

Even if $\mathscr{D}$ has already been minimized with respect to element translation and rotation, it may be possible to reduce it further by allowing extra element strain and accompanying rotation. Whereas it may be unwise to use this technique to modify original strain data, it may be worthwhile as a means of estimating either errors in the data, or unknown dilations.

If the element deforms within a rigid stationary hole, we have

$$\begin{aligned} {}_0Y_I^* &= {}_0Z_I^*, \\ {}_0Y_I^* &= D_{IJ0}Z_J, \end{aligned} \tag{16}$$

where D_{IJ} is a deformation gradient tensor for the extra strain and rotation. Substitution of (16) into (8) yields

$$\mathscr{D} = ({}_0Z_I^* - D_{IJ0}Z_J)^2 \tag{17}$$

and minimization gives

$$\frac{\partial \mathscr{D}}{\partial D_{IJ}} = 2\overline{({}_0Z_I^* - D_{IK0}Z_K)\,{}_0Z_J} = 0, \tag{18}$$

whence

$$D_{IK}\overline{({}_0Z_{K0}Z_J)} = \overline{{}_0Z_I^*{}_0Z_J}. \tag{19}$$

This is a set of linear equations in the unknown D_{IK} and can be solved by inverting the covariance matrix, $\overline{{}_0Z_{K0}Z_J}$, and premultiplying by $\overline{{}_0Z_I^*{}_0Z_J}$. The method is

formally analogous to the fitting of a first order trend surface to values of ${}_0Y_I$.

If only a dilation is permitted, we put $D_{IK} = \lambda\delta_{IK}$, where λ is the dilation, and (19) becomes

$$\lambda\overline{Z_I^2} = \overline{{}_0Z_I^*Z_I}. \tag{20}$$

The true hole and the equivalent hole

Although an element need not have the same form as the true hole enclosed by immediately adjacent elements, it is possible to define an equivalent hole whose average shape is of the same form as that of the element. Furthermore, if the element fits perfectly into the equivalent hole, it can be shown that the deviation is minimized. Thus, the equivalent hole is a useful graphical aid for judging the compatibility of an element with its neighbours.

If elements are cubic in the deformed state, they become parallelepipeds in the undeformed state, but the true holes are not parallelepipeds. For example, in the two-dimensional quadratic model (Fig. 3), the true holes are general quadrilaterals; in other examples, the true holes are more complex. Nevertheless we can define equivalent holes that are parallelepipeds (or parallelograms). One way of doing this is to consider boundary points that lie at the corners only of elements (Fig. 4). Thus, an element has 8 corners whereas its true hole has up to 24 corners (6 neighbouring elements contributing 4 corners each). By taking these corners in triplets and calculating the vector mean of each triplet, we obtain a hole with 6 faces and eight corners (Fig. 4); then, by calculating the vector means of each face, we obtain 6 face centres, defining a parallelepiped. This is the equivalent hole, into which an element is to fit.

By simple algebra involving vector means, it can be shown that the deviation $\mathscr{D}$ is a minimum when a parallelepiped and its equivalent hole have exactly the same shape and dimensions, so that the interfacial distances are zero. Thus, in the quadratic model (Fig. 3), each element is an exact image of its equivalent hole, the interfacial distances are zero, and the deviation, $\mathscr{D}$, calculated using corners, is not zero, but is a minimum.

To summarize, compatibility is considered perfect when each element is an exact image of its equivalent hole.

Numerical fitting

In previous sections it has been shown how an element can be fitted into its hole so that the deviation of one from the other is a minimum. Calculation of the required translations and rotations is a simple matter for an automatic computer, especially one whose language is adapted to handling matrices.

To pack together an array of elements, the fitting procedure is performed for the first element, all its neighbours being held fixed; then the procedure is repeated for the second element, all its neighbours, including the first element, being held fixed; and so on, until the last element has been fitted, thereby completing one cycle through the entire array. Next, another cycle is performed in the same way; and so on, for successive cycles, until further adjustments are negligible.

This packing procedure has been found to converge in all examples (about 20) studied so far, but convergence can be slow.

In some examples, instabilities have been observed, in which lines of overlapping elements buckle by rotation instead of extending uniformly by translation of individual elements; these instabilities disappear later, but hinder rapid convergence. In other examples, parts of the array become temporarily locked into metastable configurations.

For these reasons, we have devised a less accurate but fast-packing procedure, suitable for the early stages of adjustment. The procedure is analogous to crystal growth. First, a nucleus is chosen; then, a first shell of elements is packed around the nucleus, each element being fitted into the space defined by at most two other elements already consolidated; and so on for successive shells, until all the elements are consolidated. The fast-packing procedure is used for one cycle only, yet it accomplishes most of the required translations and rotations. Further fine adjustments can then be accomplished using the more complete packing procedure, described earlier. Computer programs for these procedures are being prepared for publication elsewhere.

ERRORS

Errors in a deformation field obtained by strain integration may arise in the following ways.

Integration errors

These result from the integration technique and the finite size of the elements employed. Their magnitudes may be estimated roughly, using what is known about errors in the modified Euler method of solving ordinary differential equations. Here the errors are of the order of h^3, where h is the fractional step length. Thus the use of ten elements will lead to an error of about $(0.1)^3 = 0.001$ or 0.1% in the length of a line.

If integration proceeds in more than one direction, as in the finite element technique, errors in the three directions are not independent of one another, because of the compatibility conditions (4), approximated by the minimization criterion. Thus, there may be local increases or decreases in the error magnitudes estimated above.

As in finite element solutions of mechanical problems, one way of assessing integration errors is to repeat an integration three or four times, using successively smaller element sizes, to see how much the answers differ. If the differences are negligible, it can be assumed that the elements are small enough and the answer acceptable.

So far, no tests of this kind have been attempted while integrating strains using finite elements. Clearly they are necessary, now that the technique is beginning to be used with some frequency.

Data errors

If the data are natural strains, they will inevitably be subject to errors, as a result of (i) faulty measurement, (ii) inadequate strain gauges, (iii) unknown dilations and other reasons.

If the errors are not too large and are randomly distributed in terms of spatial position and orientation, we might expect them to compensate for one another during the minimization procedure. As a simple illustration, consider an array of identical plane elements in the undeformed state (Fig. 5a). If errors of ±10% in principal strain values, but not principal orientations, are introduced (Fig. 5b), they compensate for one another almost completely during integration. Additional errors of ±10% in principal orientation are more serious (Fig. 5c), but compensation still occurs.

If errors are systematic, they will inevitably accumulate during spatial integration and this must be taken into account; but integration may yet yield the basic pattern of the deformation field and hence may be worth performing.

A measure of the magnitude of random errors may be gained by computing the total deviation using interfacial distances (not intercorner distances, as mistakenly suggested by Percevault & Cobbold 1982). The smaller the deviation, the smaller the likelihood of random data errors.

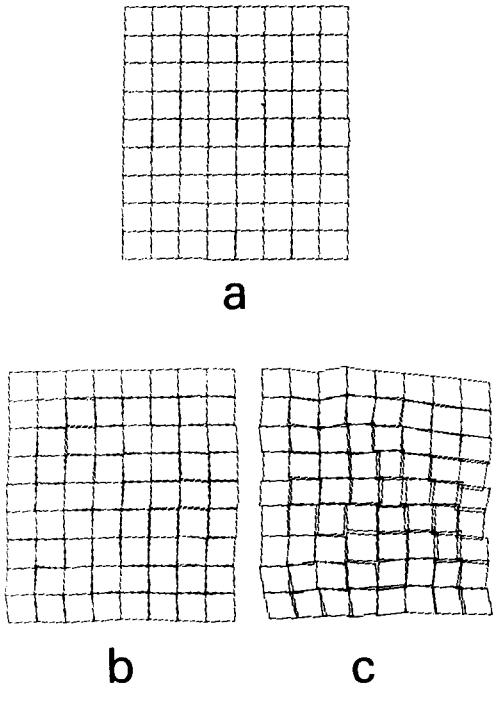

Fig. 5. Effect of errors. (a) Array of square elements in undeformed state. No errors. (b) Errors of ±10% in principal strain values. (c) Errors of ±10% in both principal values and orientations of strain.

Systematic errors, in contrast, may have but a small effect on the total deviation. In particular, a homogeneous dilation has no effect on element configuration: systematic volume change is therefore indetectable if only deviatoric strains are available as data.

To conclude this section, further work is obviously required on the effects of errors and of unknown volume changes.

CONCLUSIONS

(1) The finite element technique for spatial integration of strains is essentially equivalent to the modified Euler method for numerical integration of ordinary differential equations.

(2) It is convenient for elements to be parallelepipeds or parallelograms, as equant as possible before each is unstrained.

(3) Unstrained parallelepipeds should be fitted together by minimizing the distances between the face centres of adjoining elements.

(4) A measure of misfit between an element and the hole enclosed by its neighbours is the deviation, $\mathscr{D}$, defined as the mean square distance between points lying on the element boundary and points lying on the hole boundary.

(5) A criterion for best fitting an element in its hole is to minimize the deviation. This yields the unknown translation and rotation which the element must undergo to ensure a best fit.

(6) Fitting of an array of elements is best performed by computer: each element is fitted in turn into the hole enclosed by stationary neighbours. A fast packing routine obtains a good but approximate result after only one cycle of fitting operations. Another more rigorous routine improves the result during several further cycles of operations.

Acknowledgements—Theoretical aspects were mainly developed by P. R. Cobbold; computing by M. N. Percevault. The work forms part of the Thèse de Troisième Cycle of M. N. Percevault, who acknowledges financial support from the Direction Générale de la Recherche Scientifique et Technique, France.

REFERENCES

Cobbold, P. R. 1979. Removal of finite deformation using strain trajectories. *J. Struct. Geol.* **1**, 67–72.

Etchecopar, A. 1974. Simulation par ordinateur de la déformation progressive d'un aggrégat polycristallin. Thèse de Troisième Cycle, Université de Nantes, France.

Grioli, G. 1940. Una propietá di minimo nella cinematica delle deformazioni finite. *Boll. Un. Matematica Italiana* **2**, 452–455.

Hossack, J. R. 1978. The correction of stratigraphic sections for tectonic finite strain in the Bygdin area, Norway. *J. geol. Soc. Lond.* **135**, 229–241.

Oertel, G. 1974. Unfolding of an antiform by reversal of observed strains. *Bull. geol. Soc. Am.* **85**, 445–450.

Percevault, M. N. & Cobbold, P. R. 1982. Mathematical removal of regional ductile strains in Central Brittany: evidence for wrench tectonics. *Tectonophysics* **82**, 317–328.

Ramsay, J. G. & Graham, R. H. 1970. Strain variations in shear belts. *Can. J. Earth Sci.* **7**, 786–813.

Schwerdtner, W. M. 1977. Geometric interpretation of regional strain analyses. *Tectonophysics* **39**, 515–531.

Truesdell, C. & Toupin, R. 1960. The classical field theories. *Handbuch der Physik* (edited by Flügge, S.) **3** (1), 226–793. Springer, Berlin.

APPENDIX

Polar decomposition of an asymmetric matrix

Given a matrix $\boldsymbol{D}$, we wish to express it as the matrix product of a symmetric matrix, $\boldsymbol{S}$, and an orthogonal matrix, $\boldsymbol{O}$, as follows.

$$\boldsymbol{D} = \boldsymbol{O} \cdot \boldsymbol{S}. \tag{A1}$$

Perhaps the most obvious way of obtaining such a decomposition is to note that if we form the symmetric matrix, $\boldsymbol{C}$, given by

$$\mathbf{C} = \boldsymbol{D}' \cdot \boldsymbol{D}, \tag{A2}$$

where the dash indicates a transpose, then $\boldsymbol{S}$ and $\boldsymbol{C}$ are related (Truesdell & Toupin 1960):

$$\boldsymbol{S} = \boldsymbol{C}^{1/2}, \tag{A3}$$

so that

$$\boldsymbol{O} = \boldsymbol{D} \cdot \boldsymbol{C}^{-1/2}. \tag{A4}$$

The problem with this approach is that operation (4) involves (i) finding the proper numbers and proper vectors of $\boldsymbol{C}$; (ii) taking the reciprocal square roots of the proper numbers of $\boldsymbol{C}$ to obtain the proper numbers of $\boldsymbol{C}^{-1/2}$; (iii) forming $\boldsymbol{C}^{-1/2}$ from its proper numbers and the same proper vectors as those of $\boldsymbol{C}$. The operation is long and numerically inconvenient, as proper numbers may be difficult to extract with any accuracy, especially if one or more of them are close to zero.

The following numerical method was used instead, because it was found to be rapid, accurate and unfailing.

If we consider Cartesian components, D_{IJ}, then the components D_{12} and D_{21} can be made equal by a suitable rotation, Θ_3 about the Cartesian axis, Z_3. The angle of rotation is given by

$$\tan \Theta_3 = (D_{12} - D_{21})/(D_{11} + D_{22}) \tag{A5}$$

and the corresponding orthogonal matrix is

$$O'_{(1)} = \begin{bmatrix} 1 & 0 & 0 \\ 0 & \cos \Theta_3 & \sin \Theta_3 \\ 0 & -\sin \Theta_3 & \cos \Theta_3 \end{bmatrix}. \tag{A6}$$

On multiplying $\boldsymbol{D}$ by $O'_{(1)}$, we obtain a new $\boldsymbol{D}$, where $D_{12} = D_{21}$, but where $D_{23} \neq D_{32}$ and $D_{31} \neq D_{13}$.

Similarly, the components D_{12} and D_{31} can now be made equal by a suitable rotation, Θ_2, about axis Y_2, the corresponding orthogonal matrix being $O'_{(2)}$. On multiplying $\boldsymbol{D}$ by $O'_{(2)}$, we obtain $D_{13} = D_{31}$, but have $D_{32} \neq D_{23}$ and, once again, $D_{12} \neq D_{21}$. The difference between D_{12} and D_{21} is, however, not as great as before the operations started. Therefore if we apply a total rotation $O' = O'_{(n)} \ldots O'_{(3)} \cdot O'_{(2)} \cdot O'_{(1)}$, with components about each of the three axes in turn, $\boldsymbol{D}$ becomes symmetric and $\boldsymbol{O}'$ is the inverse of $\boldsymbol{O}$.

In practice, symmetry of $\boldsymbol{D}$ was achieved to within two decimal places after about 50 rotations about each of the Cartesian axes. This operation required about 2 min on a Hewlett-Packard Model 45 Calculator, programmed in the Basic language.